POAC'25
St. John's, Newfoundland and Labrador, Canada

Proceedings of the 28th International Conference on Port and Ocean Engineering under Arctic Conditions
Jul 13-17, 2025
St. John's, Newfoundland and Labrador
Canada

Automated Target Detection using RCM

McGuire, P.[1], Bobby, P., [1], Boyce, C., [1], Qiu, H. [1], Hetzel J. [1], Elliot B. [2], Hall R. [2]
[1] C-CORE, St. John's, Nl, Canada
[2] Equinor Canada Ltd., St. John's, Nl, Canada

ABSTRACT

Automated detection of marine targets in large volumes using RADARSAT Constellation Mission (RCM) imagery in a timely fashion requires a highly reliable process that can operate with minimal human intervention. Rapid target detection over the full dataset of appropriate images is useful for frequent updates on the locations and characteristics of the marine targets and facilitates the creation of new products to increase target confidence, aid ship/iceberg target discrimination and generate new products such as drift forecasting and target tracking. RCM data are being used to support ice management on the Grand Banks and the research is motivated to augment the current capabilities.

Recent developments at C-CORE have led to the construction of a system which automatically downloads, processes and displays targets detected in RCM imagery. The download portion of the system monitors the RCM archive for any new imagery intersecting with large geographically defined areas of interest (AOIs). Identified imagery matching a prespecified criteria (e.g. resolution, incidence angle range, etc) is acquired and processed. Part of that processing is an updated detection algorithm that provides rapid and reliable detection of small targets in dual channel SAR imagery.

INTRODUCTION

The ability to rapidly and reliably detect marine targets in satellite imagery is crucial for effective ice management, maritime surveillance, and environmental monitoring. The increasing availability of high-resolution synthetic aperture radar (SAR) data, as provided by the RADARSAT Constellation Mission (RCM), offers new opportunities for automating this process. However, efficiently processing large volumes of SAR imagery while minimizing false alarms and reducing human intervention remains a significant challenge.

To address this, we developed an advanced target detection system designed to enhance the speed and accuracy of identifying marine targets. The system automatically acquires, processes, and analyzes RCM imagery, utilizing a two-stage detection approach that combines a constant false alarm rate (CFAR) algorithm with a machine learning-based classification model. This hybrid method ensures precise target identification while controlling for ocean clutter and environmental noise.

This paper presents the key developments in the detection algorithm, including improvements in clutter modeling, target classification, and the assessment of detection probability under varying environmental conditions. The study also examines the influence of wind-induced sea state variations on target detectability and explores how different SAR parameters impact performance. By leveraging machine learning and advanced statistical modeling, the proposed system represents a significant step toward fully automated marine target detection, supporting safer and more efficient operations in Arctic and offshore environments.

DETECTION ALGORITHM

Detection and classification of targets in SAR imagery utilizes a traditional detection front-end and a machine learning classifier back-end. The front-end detection algorithm consists of the well understood CFAR (constant false alarm rate) sliding window approach, and the back end is a machine learning classifier operating on the CFAR detections (see Figure 1). The front end identifies candidate targets in the SAR imagery, one channel at a time. Each candidate detection is used to create a target "chip", a small portion of the original SAR image with the target at the center. In multi-channel SAR, the target chips are created from each of the channels regardless of which channel in which it was detected. The target chips are then formatted for use in the ML classifier which attaches a class identity and a confidence measure.

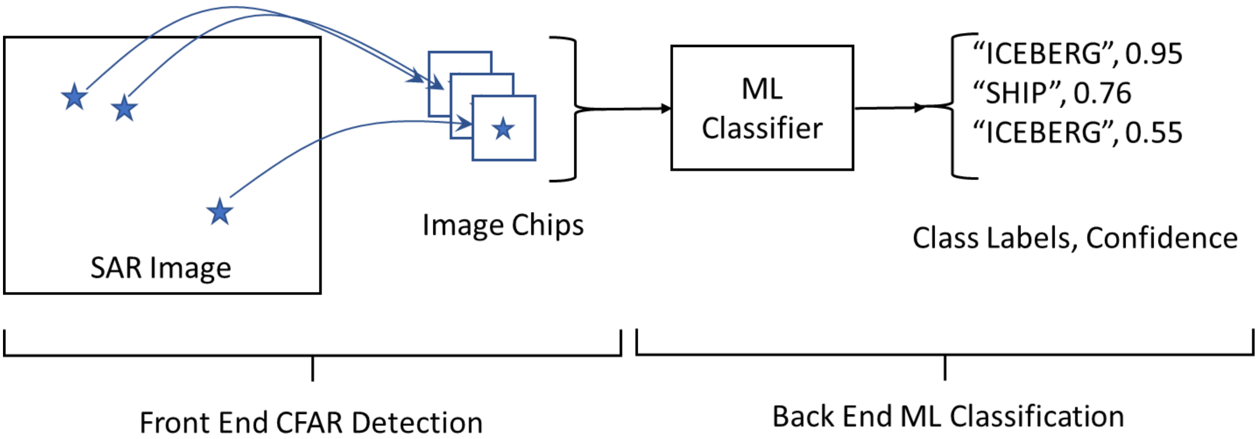

Figure 1. Detection/classification overview

This approach provides several key advantages:

- Takes advantage of CFAR detection, a well understood concept in the use of radar that provides control over the false alarm rate, i.e. the separation between target signatures and ocean clutter signatures;
- Creates a simpler problem for the ML algorithm to solve, providing comparatively better performance for a fixed data set;

- Reduces the data labelling effort required to prepare data for ML (i.e. specification of bounding boxes);
- Scales and formats image chips to increase ML target classification performance.

The following subsections detail key elements of our latest operational detection algorithm.

CFAR Detection

The detection stage consists of a sliding window CFAR algorithm, in which the ocean clutter is modelled using a probability density function (PDF) and the detection threshold is determined from the PDF (see Figure 2). The sliding window is moved across the SAR image and any returns within the window that exceed the calculated threshold are considered a detection. This method will detect any feature that is sufficiently bright in comparison to its surroundings but provides no assessment of the feature type.

The detection algorithm is controlled by two key parameters:

- Probability of false alarms (PFA): The PFA is selected to separate ocean clutter from actual targets. Smaller PFA settings result in fewer false detections but will also fail to detect smaller radar cross section targets. Typical values for this are in the range of 10^{-10} to 10^{-7}.
- Sliding window size: The sliding window must be large enough to provide a suitable statistical sample of the ocean clutter but small enough in geographical size to be considered a uniform sample. For 50 m resolution SAR our practical experience is to use a 300x300 pixel sliding window.

In our implementation we model the ocean clutter using a Gaussian PDF for intensity measurements cast in log-space. This approach differs from previous C-CORE approaches that utilize a K-distribution PDF in intensity linear space. The Gaussian approach was used because the log of the intensity measurement distribution over open ocean is adequately modelled using this PDF. The Gaussian PDF is defined using only the mean and standard deviation. In contrast, computing the K-distribution parameters requires solving a set of linear equations that are quite sensitive to outliers in the data. This sensitivity can lead to miscalculated detection thresholds, particularly when the target cross section is large. Because this issue manifests mainly on large cross section targets it is not a significant issue when manual quality control is part of the process, however this behavior cannot be tolerated in more fully automated processes.

The detection algorithm was integrated into the Coresight platform and used to process large volumes of data (i.e., 30-50 images per day). Some initial tweaking of the algorithm was performed; however, the algorithm has been operating without issue for nearly one year since that initial implementation.

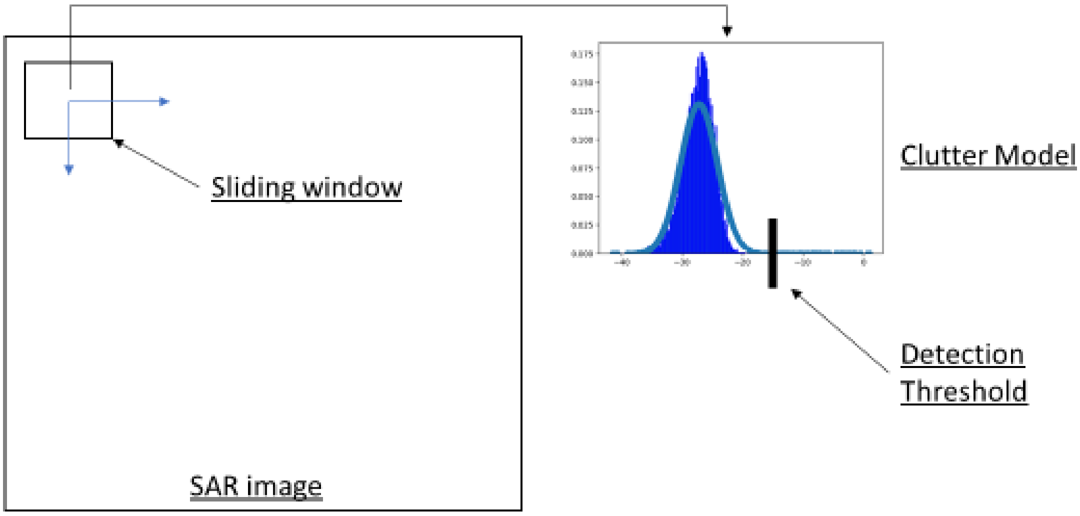

Figure 2 CFAR detection

TARGET DETECTION IN WIND

It is well known that wind conditions influence the sea state and consequently increase the scatter returns in SAR imagery. In general, the higher the winds the higher the mean return intensity. This can affect the detectability of targets.

Scatter returns due to wind conditions has been the subject of study for over 30 years. Using satellite based scatterometers a number of geophysical model functions (GMFs) have been developed to relate the mean wind vector to sigma0 returns. In this work, we refer to the CMOD7 model (Stoffelen et al. 2017). In this model the signal return is a function of windspeed, relative wind direction and incidence angle of the measurement instrument. Thus, the mean sigma0 return can be estimated for a wide range of these conditions.

In order to assess the detectability of targets in varying wind conditions, the CMOD7 model was used to make a comparison between the estimated mean clutter level and the return brightness of the iceberg targets in our database. CFAR-based target detection methods utilize peak returns to isolate targets from the background, thus for a target to be detectable the peak return must be greater than the mean clutter in the scene. Thus, in our comparison against the estimated wind clutter, the peak sigma0 value from each target signature was utilized to determine the probability of detection. The method is described below.

Target max value modelling

A dataset of 5796 iceberg targets was extracted from the larger database assembled for this project. For each target the max sigma0 return was extracted and used for the analysis. The peak value was extracted directly from the target chips themselves rather than from the database catalog. This approach made it possible to isolate the peak return in each channel (i.e. HH and HV). The distribution of peak values was used to build a probability density function (PDF) for corresponding to each channel. Since these distributions closely resembled Guassian (see Figure 3), this PDF was used.

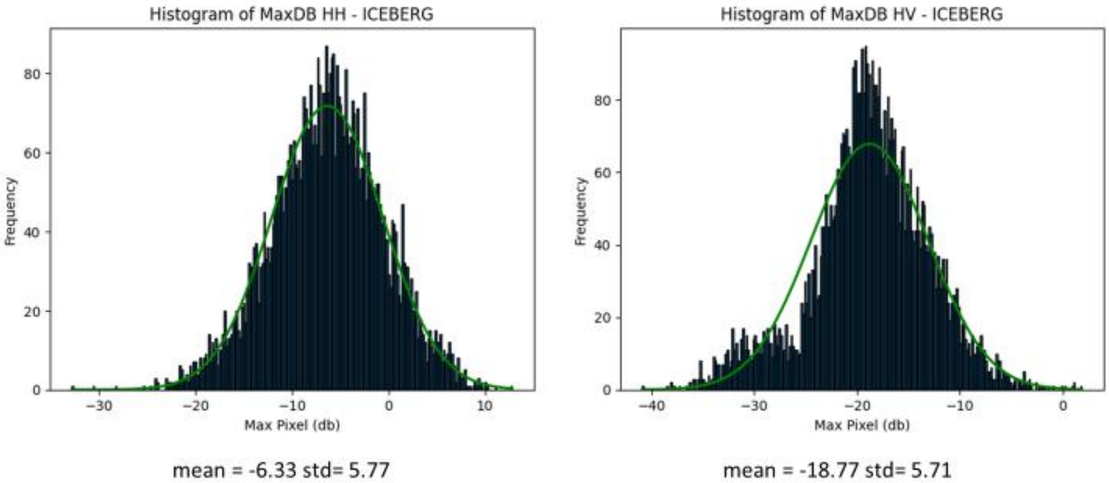

Figure 3. Distribution of max pixels in the dataset of RCM50 iceberg targets used.

A Gaussian probability density function (PDF) was created for each channel using the mean and standard deviations computed for each channel using the target database.

$$PDF(x) = \frac{1}{\sqrt{2\pi\sigma^2}} e^{-\frac{(x-\mu)^2}{2\sigma^2}}$$

Where x is the target max sigma0 value in db, and μ is the mean and σ is the standard deviation. To determine the probability P(x) of a target having a max pixel of x at incidence angle z, the PDF is integrated according to:

$$P(x,z) = 1 - \int_{-\infty}^{x} PDF(x)\,dx$$

HH and HV Channel CMOD

Vachon and Dobson (P. W. Vachon and Dobson 2000) describe a method of using polarization ratios to estimate the mean HH return corresponding to a mean VV return. In this work we utilize the Kirchoff scattering polarization ratio defined as:

$$PR^k(z) = \left[\frac{1 + 2tan^2(z)}{1 + tan^2(z)}\right]^2 \ (linear\ units)$$

The sigma0 return in HH is derived from the CMOD7 estimate in VV according to:

$$\sigma^0_{HH}(z,s,\theta) = CMOD7(z,s,\theta) - PR(z) \ \ (dB)$$

Where z is the incidence angle, s is the windspeed (m/s) and θ is the wind direction (deg) relative to the look direction, and $CMOD7(z, s, \theta)$ is the sigma0 estimate of the mean sigma0 return in VV.

Using this method, a 2D graph corresponding to a specific incidence angle can be generated. For example, Figure 4 was generated for 20 degrees incidence angle.

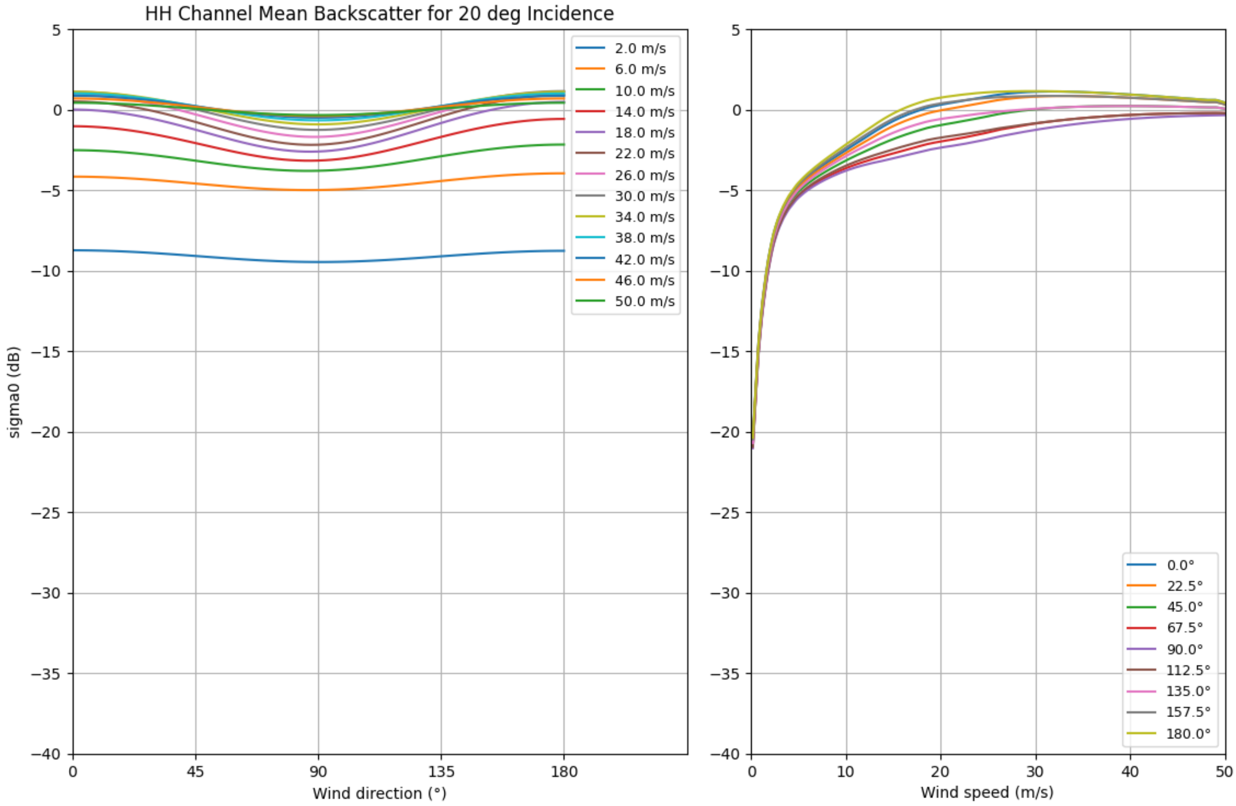

Figure 4. Mean HH sigma0 backscatter for 20 degrees incidence angle.

Vachon and Wolfe (Paris W Vachon and Wolfe 2011) describe data modelling efforts to estimate the CMOD equivalent for cross pol C-Band SAR. Their results find that the mean return in the cross pol channel is only windspeed dependent, leading to the following clutter model:

$$\sigma_{HV}^{0}(s) = 0.592s - 35.6 \quad (dB)$$

Where s is the windspeed (m/s).

Probability of detection

In order to determine the probability of detection (PoD) of a target in a given sea state, the mean clutter due to wind was compared to the probability of a target occurring with a maximum pixel value that was at least as bright as the mean clutter. Operationally, a much higher threshold is used, however this is the minimum viable threshold for target detection (albeit with many false positives).

Thus, the probability of detection (PoD) in HH for a given sea state is given by:

$$PoD_{HH}(z,s,\theta) = P(\sigma^0_{HH}(z,s,\theta),z)$$

And for HV is given by:

$$PoD_{HV}(s) = P(\sigma^0_{HV}(s))$$

Using these equations, it is possible to create PoD charts for specific incidence angles. Figure 5 and Figure 6 plot the PoD in the HH and HV channels respectively for an incidence angle of 35 degrees. Figure 7 combines these graphs to produce a 'best' PoD that represents detection using either channel at 35 degrees incidence.

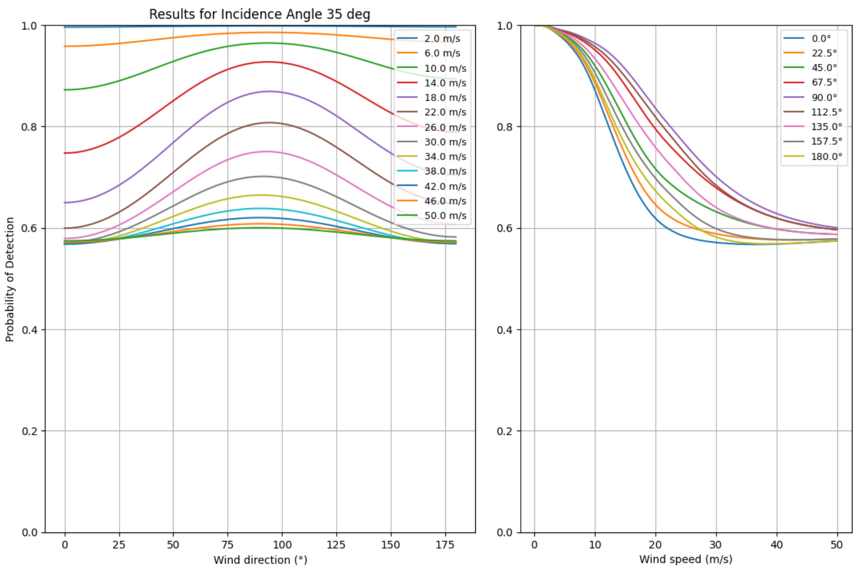

Figure 5. Probability of detection in HH at 35 degrees incidence under varying wind speeds and directions.

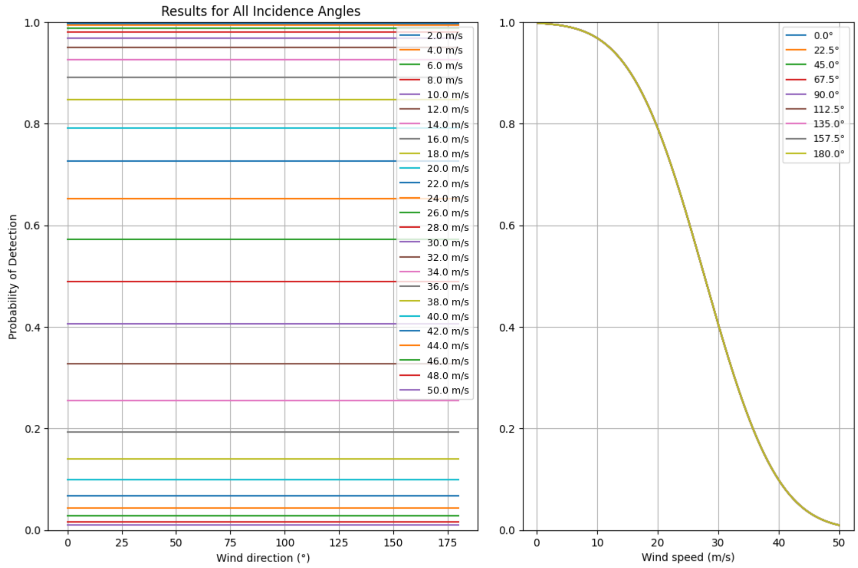

Figure 6. Probability of detection in HV at all incidence angles incidence under varying wind speeds and directions.

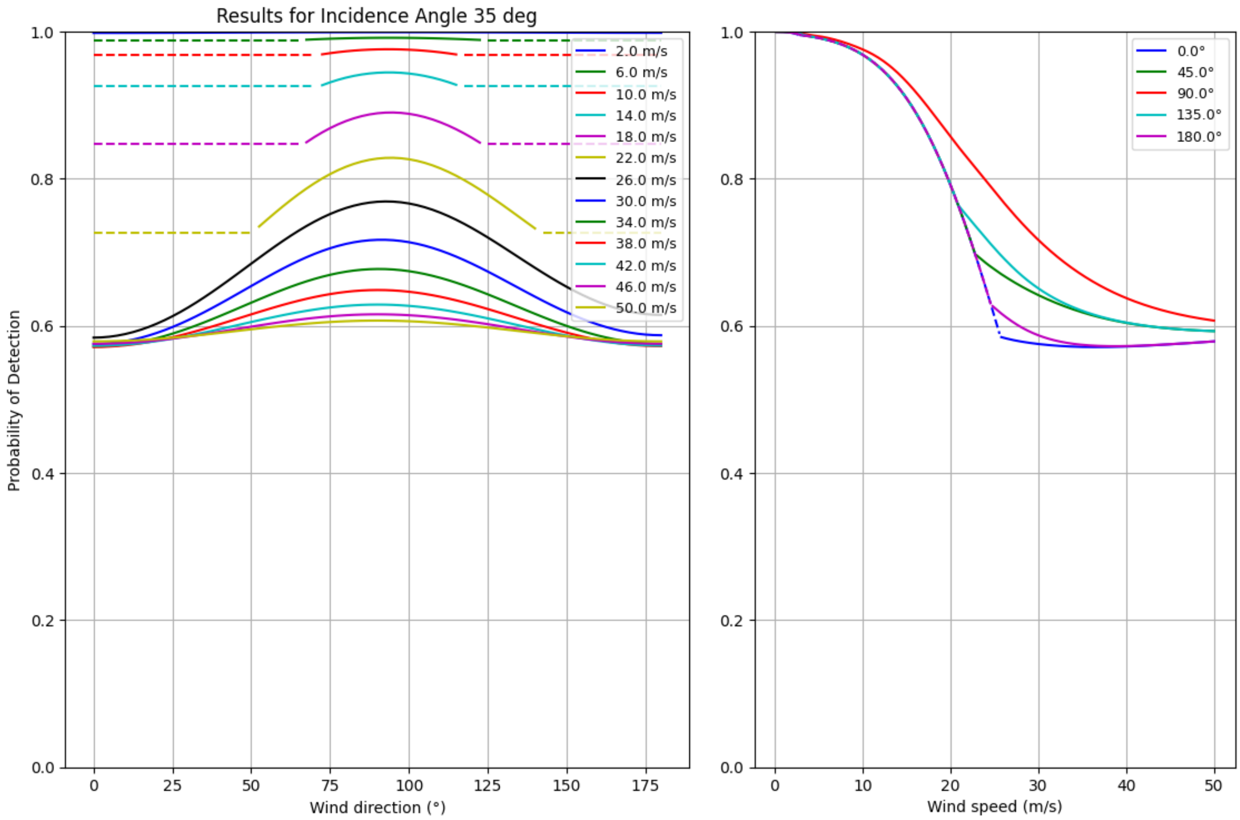

Figure 7. Best probability of detection at 35 degrees incidence under varying wind speeds and directions. Dashed lines indicate better PoD in HV, solid lines indicate better PoD in HH.

CONCLUSIONS

This study demonstrated the development and application of an automated target detection system using RADARSAT Constellation Mission (RCM) imagery. The system effectively processes large volumes of SAR data to detect and classify marine targets with minimal human intervention. By integrating a CFAR-based detection front-end with a machine learning classification back-end, the method achieves high reliability while maintaining control over false alarm rates.

A key finding from the study is the influence of wind conditions on detection probability. Using the CMOD7 model, the research quantified the impact of wind speed and direction on the detectability of iceberg targets in HH and HV polarization channels. The results confirmed that at lower incidence angles (below 35 degrees), the HV channel provides better detection performance. Additionally, the Gaussian-based clutter modeling approach proved to be more robust than previous methods, enhancing the reliability of automated detection in varying sea states.

The implementation of this automated detection algorithm into the Coresight platform has demonstrated operational effectiveness, processing up to 50 images per day with consistent performance. Future work will focus on refining the model to further improve classification accuracy and adapting the system for additional remote sensing applications.

ACKNOWLEDGEMENTS

This work was technically and financially supported by Equinor.

REFERENCES

Stoffelen, Ad, Jeroen Adriaan Verspeek, Jur Vogelzang, and Anton Verhoef. 2017. "The CMOD7 Geophysical Model Function for ASCAT and ERS Wind Retrievals." *IEEE Journal of Selected Topics in Applied Earth Observations and Remote Sensing* 10 (5): 2123–34.

Vachon, P. W., and F. W. Dobson. 2000. "Wind Retrieval from RADARSAT SAR Images: Selection of a Suitable C-Band HH Polarization Wind Retrieval Model." *Canadian Journal of Remote Sensing* 26 (4): 306–13. https://doi.org/10.1080/07038992.2000.10874781.

Vachon, Paris W, and John Wolfe. 2011. "C-Band Cross-Polarization Wind Speed Retrieval." *IEEE Geoscience and Remote Sensing Letters* 8 (3): 456–59.